

# Conceptual Aircraft Design Activities Related to Blended Wing Body Configurations in the Scope of the DLR Project SIAM

*Michael Iwanizki<sup>1</sup>, Dennis Keller<sup>2</sup>, Florian Schmidt<sup>3</sup>, Yasim Julian Hasan<sup>4</sup>, Joscha Kurz<sup>5</sup>, Felix Wienke<sup>6</sup>, Lothar Bertsch<sup>7</sup>, Michael Mößner<sup>8</sup>, Philip Balack<sup>9</sup>, Jannik Häßy<sup>10</sup>, Benjamin Fröhler<sup>11</sup>*

*<sup>1,2,3,8</sup> German Aerospace Center (DLR), Institute of Aerodynamics and Flow Technology  
Lilienthalplatz 7, 38108 Braunschweig*

*<sup>4,5</sup> German Aerospace Center (DLR), Institute of Flight Systems  
Lilienthalplatz 7, 38108 Braunschweig*

*<sup>6,7</sup> German Aerospace Center (DLR), Institute of Aerodynamics and Flow Technology  
Bunsenstraße 10, 37073 Goettingen*

*<sup>9,11</sup> German Aerospace Center (DLR), Institute of System Architectures in Aeronautics  
Hein-Saß-Weg 22, 21129 Hamburg*

*<sup>10</sup> German Aerospace Center (DLR), Institute of Propulsion Technology  
Linder Höhe, 51147 Cologne*

## Abstract

In the scope of the DLR project SIAM, new low noise concepts for short- and medium range aircraft are investigated. This paper describes the activities related to the blended wing body-type configurations. It comprises a brief project overview, the blended wing body concept background, the description of methods applied, the actual aircraft design activities and the corresponding results. The studies indicate a strong impact of handling quality requirements and of a limited high lift performance. The resulting concept is a blended wing body with a T-tail that shows a significant noise impact reduction (8-14dB) compared to an advanced tube-and-wing baseline.

## 1. Introduction

The reduction of noise emissions for future aircraft is one of the key requirements according to the Flightpath 2050 [1] (65% reduction by the year 2050 compared to aircraft in 2000). Regarding the engine as one of the main sources of noise, the increasing bypass ratio in recent decades has significantly improved both efficiency and noise. Some unconventional approaches that promise further benefits as the distributed propulsion [2] are investigated nowadays. Besides the engines, the airframe design offers several opportunities to further reduce the noise level of the aircraft. Different projects were addressing this topic in the past. Some representative examples are the DLR (German Aerospace Center) projects “Low Noise Aircraft” [3] and “KonTeKst” [4], and the international “Silent Aircraft Initiative” (SAI) [5], [6].

The DLR project SIAM (Schall-Immissions-Armes Mittelstreckflugzeug, eng: low-noise-immission medium range aircraft) is dedicated to the development of an aircraft for a typical short- and medium-range mission for entry into service in 2035 that promises a significant reduction of the noise impact. The focus is on noise immissions, meaning the noise perceived on ground.

In the first part of the project, conceptual design activities are carried out. Three design streams cover different aircraft concepts: turbofan powered tube & wing, turboprop powered tube & wing, and turbofan powered blended wing body (BWB) configurations. In this paper, the conceptual design activities specifically related to the BWB-type configurations are summarized. For the assessment of the new concepts, an advanced tube & wing baseline configuration, optimized w.r.t. fuel consumption, is provided.

## 2. Overview of the blended wing body configuration

In [7], Liebeck describes that the BWB configuration has been initially proposed to improve the efficiency of long-range large capacity transport aircraft. The basic idea was to reduce the wetted area of the aircraft by a more efficient fuselage and synergy effects related to the integration of wings, control devices and engines. Different shell designs were considered and finally, a pressure vessel with a non-circular cross-section was favored. Since then, the resulting BWB layout is utilized in many projects and adapted in different ways. Exemplary projects with DLR's contribution are listed below.

In the project VELA (Very Efficient Large Aircraft) [8] different large BWB configurations with a capacity of about 800 passengers have been developed, optimized, and evaluated. In the European project NACRE (New Aircraft Concepts Research) [9] the VELA-configuration has been further improved. In the DLR project FrEACs (Future Enhanced Aircraft Configurations) [10], the NACRE-BWB has been downsized to 450 passengers. In the scope of the Clean Sky 2 program, in the project NACOR (New innovative Aircraft Configurations and Related issues) [11], a short-and-medium range BWB for 150 passengers has been designed and evaluated. In all of these projects, an improvement in efficiency of the BWB compared to advanced tube-and-wing reference configurations was found.

The initial focus of the BWB development was on efficiency, but this concept also offers a large potential to reduce the engine noise impact by shielding [7]. Furthermore, due to the proposed low wing loading, a simple and silent high lift system can be utilized. Therefore, several projects selected the BWB for future low noise aircraft concepts ([12],[13]). The combination of a potentially silent and efficient aircraft is the reason to consider the BWB as an option in the scope of SIAM.

## 3. Methods applied

In this section, the methods applied for the design and evaluation of the BWB-type configurations in the scope of the project SIAM are described. A combination of conceptual methods (referred to as low fidelity (LoFi) methods), directly utilized for the overall aircraft design (OAD), and high fidelity (HiFi) methods, applied to increase the level of fidelity in most critical areas, is used.

### 3.1. Aircraft design workflow

A specialized aircraft design workflow is developed to automatically design a consistent aircraft and to perform design studies. The workflow is implemented in the Remote Component Environment (RCE) of DLR [14]. The architecture of the workflow is shown in Figure 1.

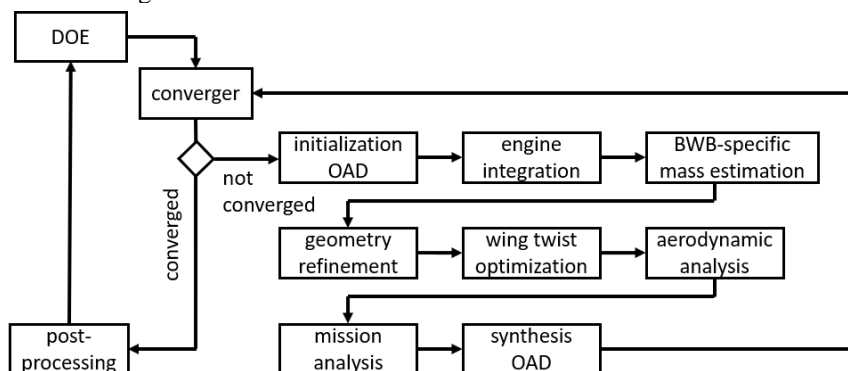


Figure 1: Overall aircraft design workflow architecture

The workflow is driven by a “design of experiments” (DOE) component that enables automated parameter studies. The “converger” component controls the iterative aircraft design process. This process is carried out until a convergence of the maximum take-off mass (MTOM) and the operating empty mass (OEM) are reached. In the initialization step, the planform of the BWB is defined based on the inputs from the DOE component. Then, an initial design of the aircraft in the “Common Parametric Aircraft Configuration Schema” (CPACS) is generated by the DLR’s semi-empirical OAD tool openAD [15]. In the next steps, the thermodynamic engine model is integrated, the mass estimation of BWB-specific components is carried out, and the geometry description of outer wing is refined. Then, the lift distribution is optimized w.r.t. the maximum L/D-ratio in mid cruise. For tailless configurations, the wing twist is adapted under consideration of the trimmed flight without a deflection of control devices. For configurations with a horizontal tailplane (HTP), the wing is optimized for maximum L/D and the HTP is used for trim. After the

optimization, aerodynamic polars are calculated. Utilizing those polars, the engine performance map, and the aircraft parameters, a mission analysis is carried out by the Aircraft Mission Calculator (AMC) [16]. AMC provides information about the fuel mass required for the design mission. All those results are synthesized, a new input for openAD is generated and a new calculation by openAD is performed. The updated results are evaluated by the “converger” component. As long as the convergence criteria are not fulfilled, new iteration loops are initiated. In case of convergence, the post-processing is initiated and the static margins at cruise condition for two most critical locations of the center of gravity (CoG) are calculated.

### **3.2. Aircraft design and data synthesis**

OpenAD [15] is a stand-alone overall aircraft design tool developed by DLR. Within the design workflow it is utilized to provide an initial aircraft design, to export the aircraft definition in the CPACS format, and to calculate the parameters that are not addressed by specialized disciplinary tools. During the subsequent design process, disciplinary tools carry out more detailed calculations related to aerodynamics, mass, and mission. At the end of the process, the corresponding results are gathered and provided to openAD. This step is referred to as synthesis. The major advantage of openAD in the scope of this work is that it considers data from higher-fidelity methods for the next design iteration.

### **3.3. Aerodynamic analysis at conceptual level**

In the conceptual design workflow, the aerodynamic polars are calculated based on simplified physical and semi-empirical methods, calibrated with HiFi-results. Two DLR in-house tools are used in the conceptual phase: *Lifting\_Line* ([17],[18]) and *Handbook\_Aero*. *Lifting\_Line* is a multi-lifting-line method for subsonic flows based on potential theory. It calculates aerodynamic force and moment coefficients in three dimensions, provides dynamic derivatives, and considers the impact of control and high lift devices (only gapless devices are treated). Due to the underlying theory, *Lifting\_Line* does not account for viscous effects. The resulting aerodynamic parameters are hence corrected by semi-empirical methods in the second step. For this purpose, *Handbook\_Aero* is used. It comprises established handbook methods [19] and extended methods developed by DLR [20]. User defined formulas can be processed in *Handbook\_Aero*, as e.g. for the wave drag correction. Both tools are coupled to the CPACS format and use directly the geometrical information from the dataset.

### **3.4. Mass estimation**

The mass estimation in the conceptual phase is mainly based on semi-empirical methods. For the center-section of the BWB, the outer wing mass and the furnishing mass, area-based methods from [8] as they were applied in [11] are utilized. Other masses are estimated by the aforementioned conceptual design tool openAD [15], i.e.: empennage, landing gear, pylons, systems, operator items. The mass of the propulsion system is provided with the engine deck.

### **3.5. Mission analysis**

For the mission analysis, the calculation of the fuel mass and the payload range diagrams, the DLR tool AMC [16] is applied. It utilizes the aerodynamic and engine performance maps provided in CPACS, and solves the equations of motions in 2D. AMC calculates a step climb profile optimized for minimum specific air range.

### **3.6. Low speed performance evaluation**

The DLR in-house tool *LSperfo* [21] is used for the evaluation of the low speed performance, particularly the calculation of the take-off field length. The analysis is based on the solution of equations of motion and computes the trajectories for take-off and landing. The tool utilizes the low speed aerodynamic polar with deflected control surfaces and the engine performance map at a maximum take-off rating. In addition, supplementary data provided by the CPACS are used.

### **3.7. Engine model**

A generic engine model for a geared unmixed turbofan envisaged for entry into service in the year 2035 is created by means of the DLR in-house virtual engine framework *GTLab* [22]. The thermodynamic cycle is selected with respect

to relevant sizing operating conditions. Engine decks are calculated that provide not only information on the fuel consumption but also on required parameters for acoustic simulations.

A unified engine model is used for all aircraft concepts to ensure a fair and consistent comparison of the airframe's impact on noise. In order to avoid unfeasible flight trajectories due to high thrust reserves, the engine is de-rated for each configuration individually by limiting the performance maps according to the minimum thrust requirements.

### 3.8. HiFi-aerodynamic analysis and calibration of LoFi-methods

The handbook methods for the estimation of the maximum clean lift coefficient ( $C_{L_{max_{clean}}}$ ), as provided in [19] utilize generalized values for the description of the planform geometry and the performance of the airfoils. It is not trivial to identify those values for a BWB wing with significantly changing sweep angles, aspect ratios, and airfoil types (supercritical at the outer wing, reflexed at the center-section). Therefore, high uncertainties are expected during the conceptual design phase. In order to reduce those uncertainties, HiFi-aerodynamic analyses on a representative BWB geometry are carried out. The results are used for the calibration of the conceptual design methods.

For the HiFi-analyses, a BWB geometry from the OAD-process is transformed to a RANS-capable CAD-geometry. The meshes are generated by the commercial tool Centaur [23]. The DLR TAU code ([24],[25]) is utilized as flow solver with the Spalart-Allmaras turbulence model [26] with rotation and curvature correction [27] being applied. For the evaluation of the low speed performance, aerodynamic calculations at angles of attack (AoA) between 0 and 48 degrees are performed. In cruise conditions, two representative angles are evaluated.

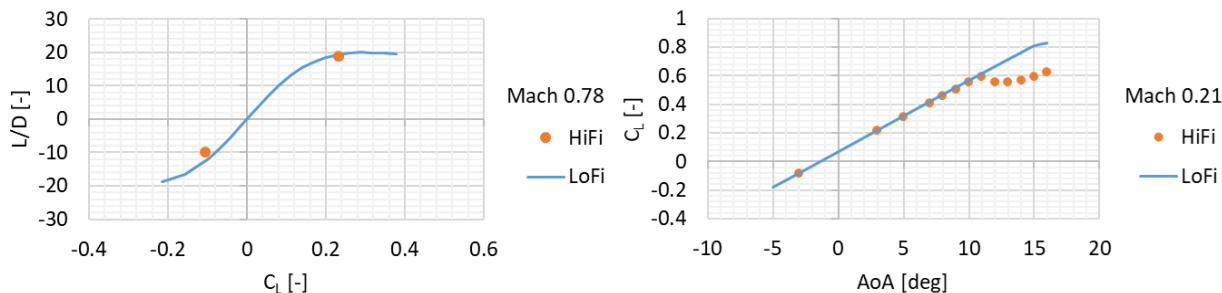


Figure 2: Comparison of HiFi and LoFi aerodynamic results for a representative BWB geometry (high-speed results the left graph, the low-speed results in the right)

In Figure 2 exemplary results are shown. At high speed, the  $L/D$ -polar shows only minor deviations between HiFi- and LoFi-calculations, especially in the region of cruise flight ( $C_L$  about 0.23). The HiFi-results in the low speed studies indicate a notable lift breakdown at an AoA of about  $12^\circ$ . Compared to the LoFi-results, this is a deviation of 25% in  $C_{L_{max_{clean}}}$ . Therefore, the LoFi-method for the estimation of the maximum clean lift coefficient is calibrated for the conceptual design studies accordingly.

The reason for the lift breakdown is a flow separation that starts at the root of the outer wing and affects the whole outboard section at higher AoA. Despite this effect, the lift coefficient further increases up an AoA of 45 degrees. This is outside of the relevant flight envelope, but it indicates a stable behaviour of the flow at the upper side of the center-section, which is advantageous for the envisaged engine installation.

### 3.9. Handling qualities and approach trajectory evaluation

Particularly for unconventional aircraft configurations, it is crucial to investigate flight mechanical aspects as early as possible in the design process, even though there are only LoFi aerodynamics and mass data available. This reduces the risk of unsatisfactory flight mechanical properties [28] that might require design changes in the later project phases. For this purpose, a handling quality investigation and a preliminary evaluation of the BWB capabilities to follow the low speed trajectories support the conceptual design phase.

Within this work, the DLR in-house flight simulation tool COAST (CPACS-Oriented Aircraft Simulation Tool) is used to automatically extract all relevant BWB aircraft data from the CPACS-file and both to generate a 6-degrees-of-freedom (6DOF) flight dynamic model and to provide a model that is linearized at the current trim point. COAST is a fixed-wing aircraft simulation framework that also provides functionalities for control allocation based on optimization, and automatic controller design [29]. The linear state-space matrices are used in the context of the handling qualities analyses. For this purpose, the DLR in-house tool HAREM (Handling Qualities Research and Evaluation using Matlab) is used, which features the assessment of a variety of handling qualities criteria for longitudinal and lateral-directional motion [30].

The 6DOF flight dynamic model is used to evaluate and ensure the fulfilment of approach and landing TLARs (airspeed, deceleration capability, 3° glideslope, wind conditions). Minimum flyable flight path angles are obtained by trimming the model for a steady descent with idle thrust and without wind. These flight path angles cover the relevant speed range, aircraft masses and aircraft configurations (high lift devices, landing gear). Afterwards the additional impact of tail-/headwind and a deceleration requirement is considered by using analytic flight mechanic equations.

### 3.10. High-fidelity fan noise shielding evaluation

One of the most dominant noise sources of an aircraft is the fan forward noise. Consequently, one of the main drivers for a quiet aircraft design is the capability for engine noise shielding towards the ground. A first estimate of the noise shielding capabilities of BWB-type configurations is obtained with the DLR solver FMCAS [31]. FMCAS uses the boundary element method to solve the wave equation in frequency domain (Helmholtz equation). The method is capable to correctly reproduce wave propagation as well as diffraction phenomena at the airframe. The sound propagation problem is solved for a quiescent medium, which still yields representative results for low Mach number flows. The sound emission of the fan is approximated by duct modes emitted at the engine inlet such that the radiation directivity of a real engine is roughly reproduced. The noise levels are evaluated far below the aircraft. The shielding effect can be visualized by first solving for an uninstalled engine without aircraft geometry and then comparing the results to the solutions of an installed engine. The goal of this high-fidelity assessment is to generate a basic understanding of the vehicles properties and to help understand the impact of the noise shielding.

### 3.11. Noise evaluation

The aircraft noise is assessed along the trajectories of a low-drag-low-power approach and an ICAO-A departure, which is generated by DLR's Flight Paths for Noise Analysis (FlipNA) tool [32]. All required operational parameters are computed with FlipNA for a subsequent noise simulation of the overall aircraft. The aircraft noise levels for receiver positions on the ground are calculated using DLR's Parametric Aircraft Noise Analysis Module (PANAM) [33]. It predicts the emissions of the relevant aircraft noise sources using a set of semi-empirical models and propagates them to the receivers. An additional attenuation of the fan noise source due to structural shielding is calculated by DLR's software SHADOW [34]. This tool is based on a ray-tracing algorithm combined with a diffraction correction. The tool applies similar simplifications as FMCAS, i.e., no-flow conditions, and provides comprehensive and representative results. The receivers are positioned below and at a parallel offset to the flight trajectories at a distance of 450 m to capture relevant areas for the noise certification of transport aircraft. An estimate of the ICAO ANNEX 16 noise certification levels is simulated, i.e., not accounting for the detailed regulations with respect to the flight conditions. The simplified assessment yields robust and comprehensive results for a comparative assessment, but absolute levels cannot readily be compared to published certification levels of existing aircraft. The additional effort for such a virtual certification as described in [35] is not required for the purpose of this work with the main focus on level differences.

## 4. Top-level aircraft requirements and baseline aircraft

The top-level aircraft requirements (TLARs) in SIAM are based on the Airbus A320 [36] configuration under consideration of [37] and [38] regarding the approach speed and the wing span limitation. The major TLARs are summarized in Table 1. In addition, a glide path angle between 3° and 4.5° is required, and the configuration shall remain stable and controllable without artificial augmentation at all loading conditions.

Table 1: Top level aircraft requirements

	<b>Unit</b>	<b>Value</b>
Design payload	t	17.1
Design range	nm	2600
Cruise Mach number	-	0.78
Take-off field length	m	< 2200
Landing field length	m	< 1800
Approach speed category C	kts	< 141
Span Limit ICAO Code C	m	< 36

The baseline aircraft is an evolutionary design of an A320-based tube-and-wing configurations for entry into service in 2035. It serves as the reference for the evaluation of the efficiency and the noise reduction potential of the unconventional concepts. For the baseline, advanced materials are utilized for the airframe and an ultra-high bypass ratio engine is installed. Furthermore, it is equipped with airframe noise reduction technologies from the project Low Noise ATRA [39]. The aircraft is optimized for minimum fuel consumption. The major aircraft data is summarized in Table 2.

Table 2: Baseline configuration data

	Unit	Value
MTOM	t	74.2
OEM	t	43.2
L/D	-	17.5
block fuel design mission	t	11.6
block fuel study mission	t	3.8

## 5. Design of the blended wing body configuration

In this section, the design activities related to the SIAM-BWB configuration are described.

### 5.1. Definition of the BWB configuration

For the initialization of the design process, a basic layout of the BWB configuration is pre-defined. The design of the center-section, meaning the planform and the airfoils, is based on the work in [11]. Both the cabin and the cargo compartment are located on the same deck, as shown in Figure 3. The generic arrangement of the control devices is also shown in Figure 3. For the handling quality and low speed trajectory evaluation, different combinations of those control devices are applied.

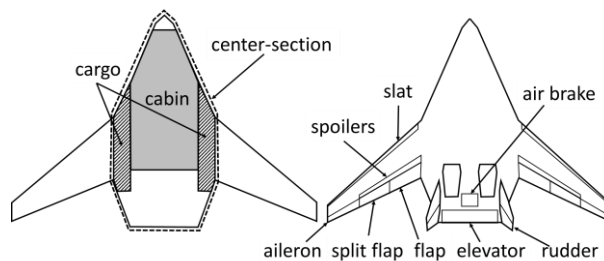


Figure 3: Cabin and cargo arrangement, control devices of the BWB

The engines are installed directly behind the pressure bulkhead of the cabin. Two vertical tailplanes (VTP) are placed at the rear of the center-section. Besides the stability and controllability aspects they also contribute to noise shielding. Since the BWB is very sensitive to the CoG travel, additional trim tanks in the front of the center-body are assumed. A detailed design at this stage has not been conducted, but the single deck arrangement offers a sufficient volume below the cabin.

### 5.2. Maximum lift and wing loading variation

According to chapter 3.8, the maximum lift coefficient of the BWB configuration is rather limited. The utilization of a powerful high lift system is barely possible, because the movables at the trailing edge are located behind the CoG and would generate a nose-down pitching moment. Also, a complex high lift system might increase the noise emissions due to gaps and is therefore avoided in the scope of this project. Finally, for trimmed flight in case of a naturally stable configuration, the elevator or the elevons have to provide downforce in order to compensate the pitching moment of flaps and thus reduce the maximum lift coefficient even further. In consequence, the low maximum lift coefficient has to be compensated by a low wing loading to provide the low speed performance required. The wing loading at the same time strongly impacts the mass and the efficiency of the aircraft.

As described in chapter 3.8, the  $C_{L_{max_{clean}}}$  is evaluated by HiFi aerodynamic analyses. It is considered conservative, since no HiFi-optimization has been conducted. In order to investigate the impact of the potential increase in maximum

lift in combination with an increase in wing loading, a sensitivity study is carried out. In Figure 4, the impact on mass and performance is shown. The wing loading is adapted for a comparable approach speed in this study. One can observe that a 10% higher maximum lift coefficient allows an increase in wing loading by about 4-5%. This improves the L/D-ratio and reduces the mass, and in consequence leads to a reduction in block fuel by more than 10%. Further improvement in maximum lift reduces the gains but still provides large benefits.

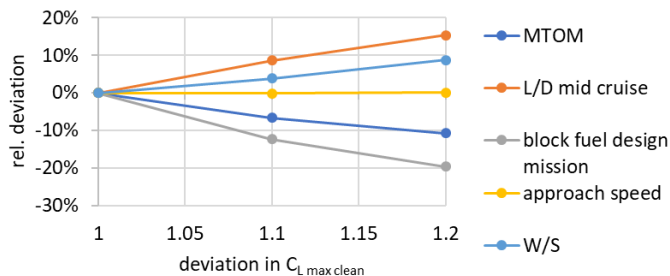


Figure 4: Variation of the maximum lift coefficient and wing loading for the BWB

### 5.3. Planform variation

In the scope of this project, the stability and controllability of the aircraft without artificial support at all CoG-locations is required. In order to identify feasible configurations during the conceptual design, the longitudinal stability is evaluated at the most critical CoG-locations at cruise conditions: design load condition (maximum forward CoG) and ferry mission without payload (maximum aft CoG). A positive minimum static margin (SM) serves as a preliminary parameter for the definition of the design space. The final assessment is carried out by detailed handling quality analyses.

The following parameter study covers different wing sweep angles and locations of the outer wing root. It shows the impact of the SM on the design space and the impact on the aircraft efficiency (Figure 5).

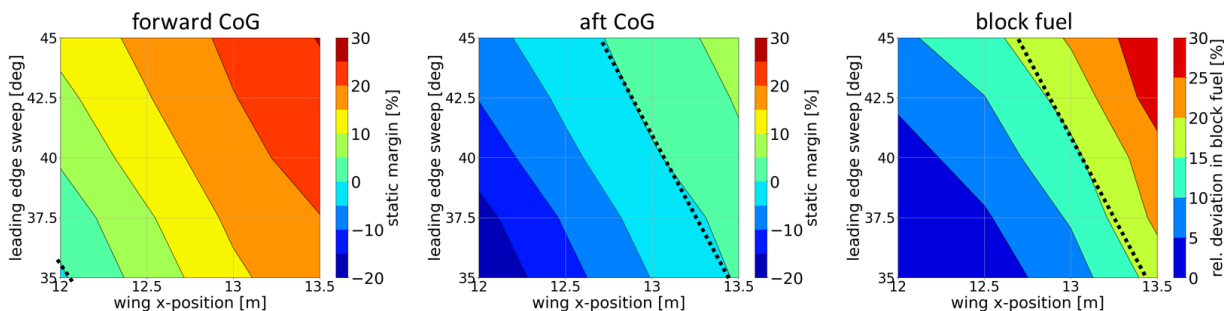


Figure 5: Impact of static margin on efficiency: SM at forward CoG, SM at aft CoG, rel. deviation in block fuel

Comparing the SM at the design load condition and the minimum SM (no payload, maximum aft CoG-location) one can observe that the minimum SM notably limits the design space. One can also observe that higher SM increase the block fuel consumption significantly (penalties higher than 10%). A major reason for it is the unfavorable lift distribution required for trimmed flight of a nose heavy tailless aircraft. The pitching moment is compensated at the cost of the aerodynamic efficiency. Therefore, one can conclude that the requirement for a naturally stable aircraft at all loading conditions significantly reduces the efficiency of the proposed BWB configuration.

### 5.4. Handling quality assessment and approach trajectory evaluation

As part of the conceptual BWB design support, detailed handling quality analyses are carried out on a representative BWB configuration presented in the studies above. Figure 6 exemplarily shows the results of two selected criteria. These are the CAP (Control Anticipation Parameter)-criterion on the left-hand side, evaluating the pitch controllability of the aircraft, and a stability criterion for the Dutch roll on the right-hand side. The results indicate a satisfactory pitch controllability at cruise at design load conditions (The point is located within the “Level 1“-band). At approach combined with the rearmost CoG location, the aircraft, however, shows a too sluggish behavior (point in “Level>3“-region), which is unacceptable in the scope of this project. The Dutch roll is still stable for both flight points, as shown in the plot on the right-hand side. At take-off, the control authority is insufficient to achieve a trimmed state in the longitudinal direction, therefore no handling quality results are available for this flight point.

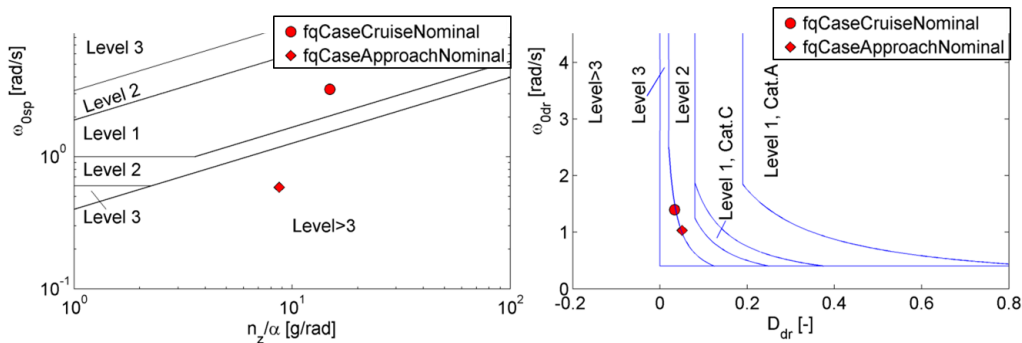


Figure 6: Handling quality evaluation for the BWB

Furthermore, the flight performance during approach is assessed. In general, the BWB has a comparably high L/D-ratio, also at low speed conditions. This causes challenges related to the glide path angle, deceleration and a stable approach. Approaches with low landing masses and tailwind are affected in particular. In order to assess the feasibility of low speed trajectories, minimum flyable flight path angles are estimated considering combinations of different airspeeds, aircraft masses, wind conditions, aircraft configurations and deceleration requirements.

The first analyses showed that it is impossible to follow at least a standard  $3^\circ$  glideslope without the utilization of aerodynamic brakes. Besides the low airframe drag, a comparably high idle thrust of the high bypass ratio engines is identified as an issue. Different devices have been considered to increase the drag. The differential deployment of the inner and central flaps (increased induced drag) did not lead to satisfactory flight path angles. Split flaps or a dedicated air brake appeared to be more promising. For this project, the devices at the upper side of the wing or center-section are preferred in terms of low noise immissions.

### 5.5. Fan noise shielding study

For the basic and high-fidelity evaluation of the noise shielding by the airframe, three BWB planforms with different lengths of the center-section are investigated with the tool FMCAS. As sound source serves a simple duct mode pattern at the engine inlet (azimuthal mode order is 18, radial mode order is 1) which is cut-on at the considered frequency of 1kHz. While a real engine has a much more complex radiation behavior, the results can give a first idea of the shielding capabilities of the BWB. Only one engine was installed to show the airframe shielding of an engine to the left and to the right of the aircraft. In Figure 7 the comparison between the uninstalled engine and the engine above the corresponding BWB configurations is presented. The color indicates the sound pressure level 50 meters below the aircraft at 1 kHz. While absolute levels cannot be evaluated due to the missing amplitude information, it is observed that the loud regions in front of the engine are completely eliminated. Sideways the sound attenuation is weaker, but still visible. The effect of the center-section length is comparably small, however, for rearward engine noise radiation it is expected to be more significant.

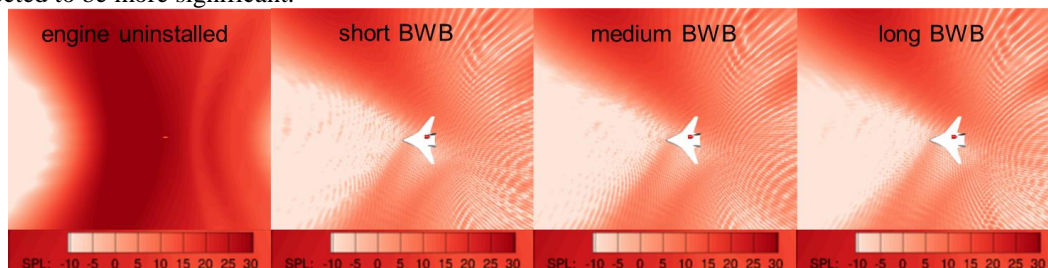


Figure 7: Impact of engine installation on noise 50 m below the aircraft (sound pressure level at 1kHz)

### 5.6. Results of the BWB configuration and related conclusions

The aforementioned HiFi simulation confirms a promising noise reduction potential of the BWB. At the same time, the low maximum lift coefficient and the wide travel of the CoG depending on the loading conditions combined with the handling quality requirements diminish the efficiency of the design significantly. Actually, none of the configurations from the aforementioned studies can fulfill all the project requirements. Therefore, highly optimistic assumptions are made for the following BWB design: relaxed static stability (longitudinal stability only at design conditions), an improvement of the maximum lift coefficient by 20%. The wing loading is adapted to meet the low-speed requirements as the field performance and the approach speed. The resulting BWB is compared to the tube-and-



wing baseline configuration in Figure 8. One can observe, that despite the optimistic assumptions the BWB is heavier and less efficient w.r.t. the fuel consumption and aerodynamic performance (L/D) than the baseline. Since the handling quality requirement is more or less neglected for this BWB, the major reasons for the inferior performance are the low speed requirements combined with a low maximum lift coefficient. This leads to an aircraft with at comparably large wing area.

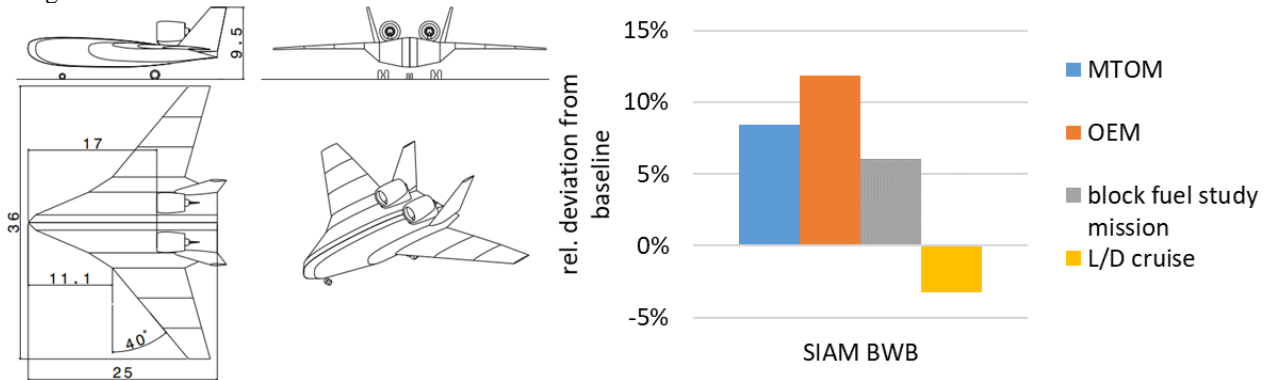


Figure 8: “Optimistic” BWB configuration and the comparison to the baseline

Since several TLARs are not fulfilled by this BWB concept, it is not applicable for the final down-selection in the project. Nevertheless, the significant engine noise shielding capability remains very attractive for a low noise aircraft concept. In order to provide a competitive BWB-type configuration, it was decided to improve the stability properties and to enable the integration of a high lift system by the utilization of a horizontal stabilizer. The corresponding design activities are described in the next section.

## 6. Design of the hybrid wing body configuration

In this section, the design activities related to the so-called hybrid wing body (HWB) configuration in the scope of the project SIAM and the corresponding results are described.

### 6.1. Definition of the HWB configuration

As mentioned before, the utilization of a horizontal stabilizer is envisaged in order to improve the handling qualities and to enable higher maximum lift coefficients by the integration of a high lift system on a BWB. In the first step, an appropriate arrangement of the HTP is selected. Three potential concepts are considered for this purpose (Figure 9): conventional tail, canard, T-tail.

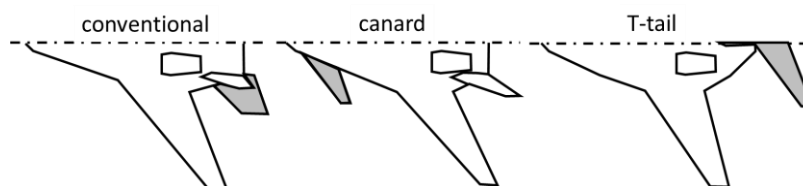


Figure 9: Options for the integration of the horizontal stabilizer for the BWB

The conventional tail configuration offers the advantages of higher elevator forces and an additional rearward noise shielding. The disadvantages are the location of the tailplane in the wake of the wing and the short lever arm. The short lever arm requires the downforce to be high in order to compensate the pitching moment of the flaps. Therefore, the lift generated by the flaps is significantly counteracted by the deployment of the elevator.

The canard offers a comparably large lever arm and advantageous shielding capabilities remain as for the “classical” BWB. The maximum lift performance of a canard configuration is expected to be lower than for a rear mounted horizontal stabilizer due to reasons described in [19], and the longitudinal stability remains challenging.

The T-tail configuration offers the advantage of a longer lever arm for the HTP, especially because it is mounted on top of a backward-swept VTP. The vertical separation between the HTP and the wing provides clean flow conditions improving the efficiency. This configuration offers the highest high lift performance of all concepts proposed. The main disadvantage of the T-tail is from acoustic perspective the additional surfaces that reflect the noise to the sides and to the ground.

Based on this qualitative evaluation, the T-tail configuration has been selected as the most promising (and conservative) for further work. This configuration is referred to as the “Hybrid Wing Body” (HWB) in this paper, due to its similarity to the HWB concept of Lockheed-Martin and NASA [40]. On the contrary to Lockheed’s concept, the SIAM-HWB has only a non-circular pressurized cabin section.

The single deck design of the BWB and the engine locations are also applied for the HWB. The rear, non-pressurized part of the center-section is extended in order to further increase the lever arm of the horizontal tailplane. A conventional layout of control and high lift devices is chosen, since the pitching moment of the flaps can be fully compensated by the HTP. In order to reduce the noise impact, a slotless high lift system is utilized. Additional air brakes are implemented at the rear of the center-section in order to enable a satisfactory flight-path angle. Although, the HWB is less critical w.r.t. the CoG travel, for the fuel system the same assumptions are made as for the BWB configuration. An overview of the HWB layout, the cabin arrangement and the control devices are shown in Figure 10.

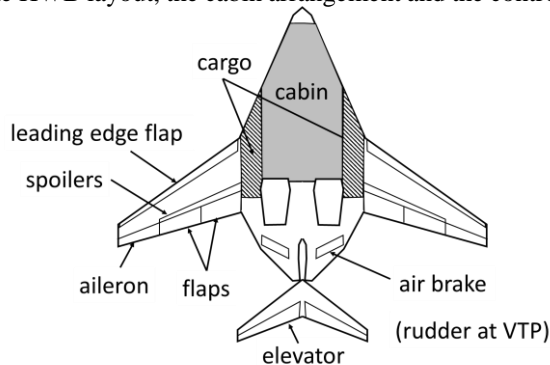


Figure 10: Layout of the SIAM-HWB configuration

## 6.2. Planform variation

As for the BWB, the planform of the HWB impacts the performance, the efficiency and the stability of the aircraft significantly. An additional degree of freedom for HWB is the length of the center section. The impact of the center-section length at aircraft level is shown in Figure 11. For this study, the wing loading has been adapted for a comparable approach speed.

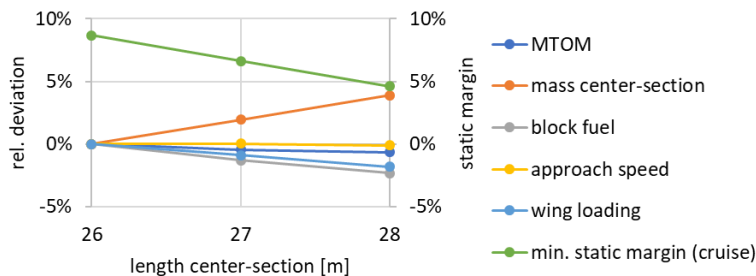


Figure 11: Impact of the center-section length at aircraft level

The results indicate that the mass of the center-section grows, the block fuel is reduced and the MTOM shows only a minor variation with an increasing length of the center-section. In order to achieve the approach speed required, the wing loading is reduced for longer center-sections. Otherwise the increasing area of the center-section leads to a reduced area of the outer wing that is crucial for the maximum lift performance, since the high lift devices are located there. Overall, a longer center-section appears to be advantageous in terms of efficiency. From the perspective of flight mechanics, the static margin is reduced by longer center-sections. For simplicity, the tail volume coefficient is kept constant during this study. The size of the HTP would have to be adapted separately in a subsequent step in order to achieve the stability required. A larger tailplane would in consequence reduce the efficiency gains of configurations with longer center-sections.

## 6.3. Maximum lift and wing loading variation

As for the BWB configuration, a generic parameter study related to the variation of the maximum lift coefficient of the clean configuration is carried out. The wing loading is adapted to keep the approach speed approximately constant.

The impact on the aircraft stability is neglected. In Figure 12 one can observe that an improvement in  $C_{L_{max_{clean}}}$  by 10% leads to a reduction in block fuel by about 5%. It is obvious that the HWB shows a lower sensitivity w.r.t the maximum clean lift coefficient than the BWB. The reason is the significant contribution of the high lift system to the total maximum lift coefficient.

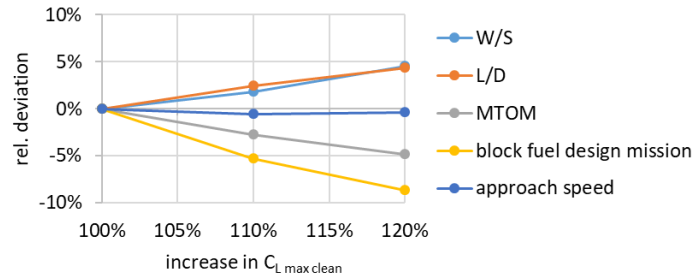


Figure 12: Variation of the maximum clean lift coefficient for the HWB

#### 6.4. HTP area variation

For the HWB configuration, the longitudinal stability is mainly achieved by the appropriate sizing of the HTP. In Figure 13, the quantitative results of a generic study addressing the HTP area are shown. As expected, a larger HTP improves the stability but decreases the efficiency of the aircraft. According to the advanced handling quality assessment, the largest HTP in this study is sufficient to provide the handling qualities required. The corresponding minimum static margin is used as reference during the conceptual design activities.

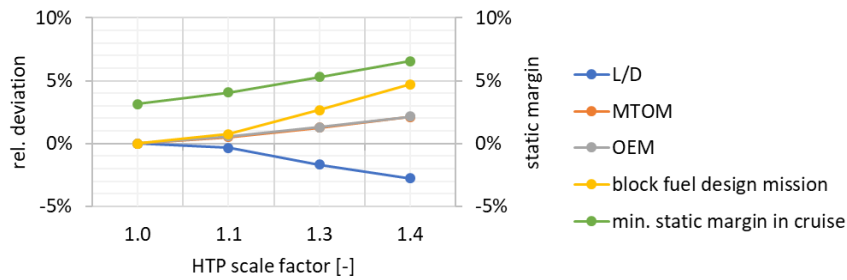


Figure 13: Variation of the HTP area for the HWB

#### 6.5. Handling quality assessment and approach trajectory evaluation

With an appropriately sized HTP, the HWB achieves acceptable handling qualities. As Figure 14 shows exemplarily for two criteria, the HTP improves to the aircraft's pitch authority and leads to an acceptable pitch controllability (point in "Level 2"-band) at all flight points.

The low-speed trajectory evaluation shows that in order to achieve the minimum flight path angle requirement ( $3^\circ$  glideslope), the spoilers at the rear of the center-section have to be deployed as air brakes.

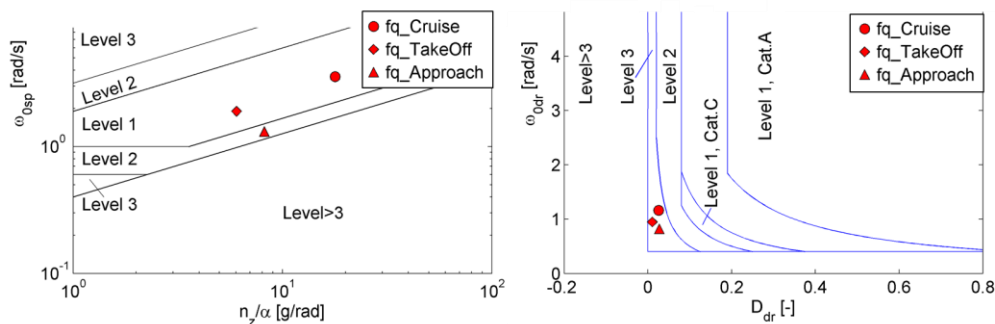


Figure 14: Handling quality evaluation for the HWB

## 6.6. Fan noise shielding

The same analysis as described for the BWB in chapter 5.5 is carried out for the HWB. In Figure 15, the sound pressure level pattern 50 m below the aircraft for a frequency of 1kHz is shown. On the left, the impact of the uninstalled engine is depicted. On the right, the engine is installed above a representative HWB geometry. The characteristics of the fan noise shielding by the HWB is similar to the BWB. A closer look reveals the negative effects of the T-tail. Nevertheless, the concept remains very promising w.r.t. the reduction of noise emissions towards the ground.

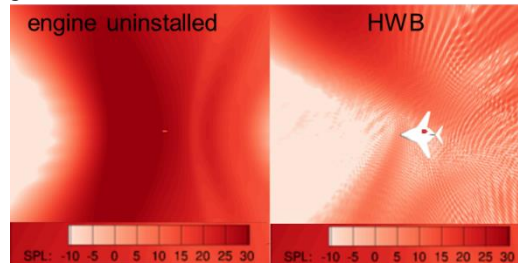


Figure 15: Impact of engine installation on noise 50 m below the aircraft (sound pressure level at 1kHz)

The HiFi-simulations are also performed in order to confirm the results of the low-fidelity tool SHADOW that is applied for the overall assessment. A good agreement with the HiFi results is found.

## 6.7. Results of the HWB configuration

Based on the aforementioned studies, the design of the HWB configuration is carried out. For the final down-selection in the project, two HWB configurations are provided. The first, so called conservative version, is based on the conservative assumptions related to the  $C_{L_{max_{clean}}}$ . The conservative approach is not typical in the scope of OAD, but meaningful for the risk mitigation regarding subsequent project activities. For the second, so called optimistic version, a moderate improvement of  $C_{L_{max_{clean}}}$  by 10% is assumed. The higher lift coefficient allows an increase of the wing loading by 1.8% compared to the conservative variant. To meet the minimum static margin requirement, the tail volume coefficient for the HTP is also increased by 12%. In Figure 16, the three-views of both HWBs are shown.

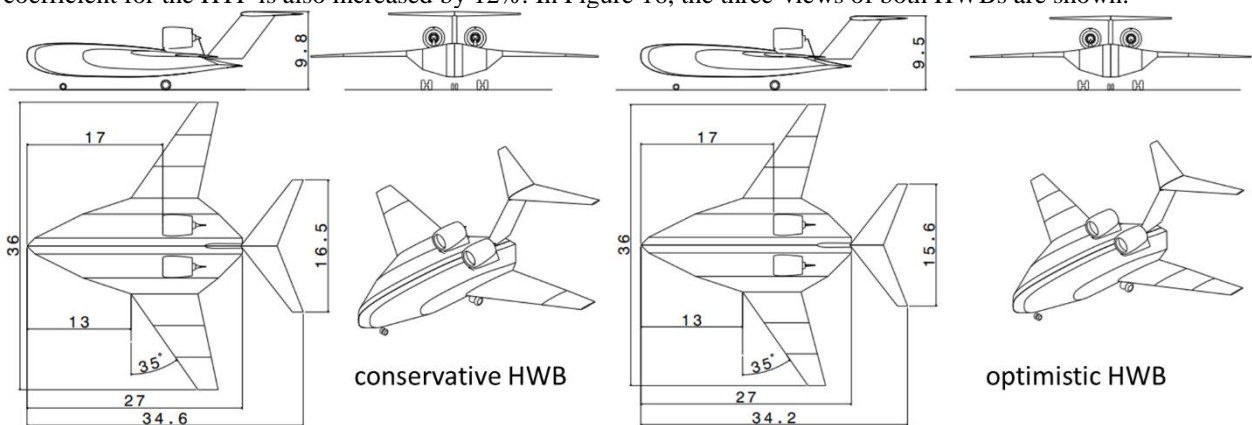


Figure 16: Overview of HWB configurations

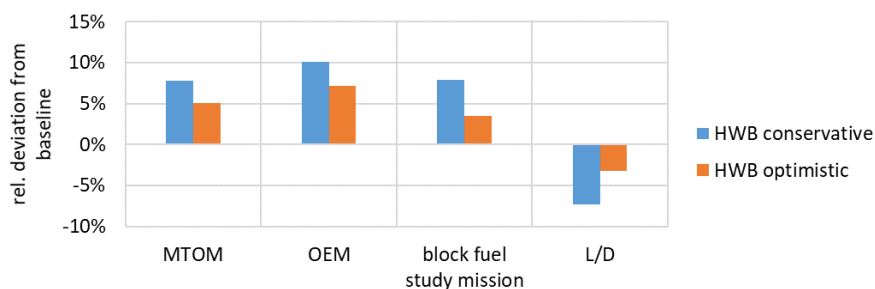


Figure 17: Comparison of the final HWB concepts to the baseline w.r.t. mass and efficiency

In Figure 17, the comparison between the two final HWB configurations and the baseline is drawn. One can observe that both HWBs are heavier in terms of MTOM and OEM and are less efficient in terms of aerodynamics and fuel consumption. The hypothetical increase of the maximum clean lift coefficient by 10% shows a significant performance improvement. The optimistic configuration reduces the penalty in block fuel from 7% to 3%. By the utilization of a more powerful high lift system, even further improvement in efficiency is considered possible. This would have to be traded against additional noise sources.

The simplified certification noise evaluation at three certification points (flyover, approach, and side line) is shown in Figure 18. For the baseline configuration, the low-noise measures of the project Low Noise ATRA [39] are accounted for. The HWB concepts are equipped with a slotless high lift system, which is approximated by a level reduction of 5 dB for flap and slat noise. This is in good agreement with earlier works on such concepts as described in [41].

In Figure 18, a significant advantage of the HWB configuration over the reference tube-and-wing layout with underwing engines becomes obvious. At the flyover point, the highest noise reduction of about 13 dB-14 dB is identified. At the side line and the approach points a reduction of about 8-9dB is obtained. The assumptions regarding the maximum lift coefficient do not notably impact the magnitude of the noise reduction.

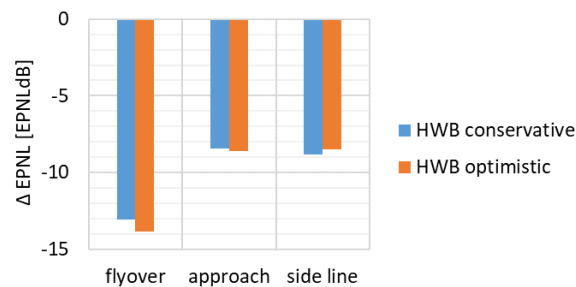


Figure 18: Comparison of HWB concepts and the baseline w.r.t. noise

## 7. Summary

In the scope of the DLR project SIAM, a low noise aircraft configuration is developed. In the first phase, conceptual design studies of tube & wing and blended wing body (BWB) configurations are carried out. The most promising of those concepts shall be selected as the basis for the subsequent project activities. In this paper, the design work related to different BWB-type configurations during the conceptual design phase is described.

For the conceptual design activities semi-empirical and low-level physics-based methods are utilized. In addition, HiFi-aerodynamic calculations are carried out for a representative configuration in order to enable the calibration of the LoFi-methods. The handling qualities are evaluated by detailed physics-based methods. A simplified noise certification assessment is carried out by conceptual methods and also cross checked with HiFi-results.

The design mission, the field performance, and the approach speed category are based on an Airbus A320-type aircraft. The entry into service is envisaged for 2035. A specific project requirement is that the aircraft has to remain stable and controllable without an artificial stability system.

The basic layout of the BWB is based on the DLR work previously carried out in the scope of Clean Sky 2. The resulting SIAM configuration has a single deck layout and engines mounted at the upper side of the center-section, behind the pressurized section. The engine model is based on a thermodynamic design process. The conceptual studies of the BWB configuration comprise the wing loading, the wing planform, and the maximum lift coefficient. The parameter studies indicate strong limitations for the BWB due to the poor high lift performance and the restrictive handling quality requirements. The resulting BWB concept offers significant engine noise shielding capabilities, but even with a relaxed stability margin, it remains less efficient than the tube & wing baseline configuration. Therefore, a BWB configuration with a horizontal tailplane is introduced, referred to as “hybrid wing body” (HWB). The design process of the HWB comprises similar studies as for the BWB and in addition the size of the tailplane. Two final HWB configurations with different assumptions for the maximum lift performance are proposed. Both are less efficient w.r.t. the fuel consumption than the tube and wing baseline (3% and 7%). But they offer a notable noise impact reduction at all certification points (8 dB-14 dB).

## 8. Conclusions

The short- and medium-range hybrid wing body configuration (HWB) developed in the scope of this work offers significant noise reduction potential (8 dB-14 dB depending on the certification point) compared to the conventional tube-and-wing baseline configuration. The design of the HWB is a consequence from studies with “classical” BWB

configurations that could not fulfill several project requirements due to handling quality and maximum lift issues. The HWB is designed as a naturally stable aircraft that is controllable without artificial support. Assuming that for the certification in future the aircraft would have to remain controllable in case of the flight control system failure, the HWB would be a more feasible concept than an inherently unstable BWB. The efficiency of the two proposed HWBs in term of fuel consumption is inferior compared to the baseline configuration (3%-7%). The reasons are the high structural mass and a low maximum lift coefficient. There is a high probability that by HiFi-optimization the maximum lift coefficient of the clean configuration could be increased. Also, the integration of a more powerful high lift system is more feasible for the HWB than for the BWB configuration due to the pitching moment authority of the horizontal stabilizer. In consequence, the HWB concept offers further optimization potential for both, noise and fuel efficiency. Nevertheless, there are several remaining uncertainties related to this concept. The cabin design of the BWB-type configurations remains challenging w.r.t. the ground operations, evacuation, and passenger comfort. The detailed investigations of those aspects were out of the scope of this project. Hence, a feasible cabin arrangement proposed in the scope of the Clean Sky 2 project NACOR has been utilized in the first step. The mass estimation methods applied are comparably simple and remain a significant point of uncertainty. Especially the pressurized, non-circular cabin cross section bares the highest uncertainties. This would have to be addressed by HiFi methods, since no reference data from existing aircraft is applicable.

## References

- [1] European Commission, Directorate-General for Mobility and Transport, Directorate-General for Research and Innovation, Flightpath 2050: Europe's vision for aviation: maintaining global leadership and serving society's needs, Publications Office, 2011, <https://data.europa.eu/doi/10.2777/50266>
- [2] Hall, C. A., & Crichton, D. (2005). Engine and installation configurations for a silent aircraft. ISABE, 1164, 2005
- [3] Lummer, M., Hepperle, M., Delfs, J. W., & Kresse, N. (2004). Towards a Tool for the Noise Assessment of Aircraft Configurations. In Proceedings of the 8th ASC-CEAS aeroacoustics workshop
- [4] Krengel, M. D., Bertsch, L., Dahlmann, K., Günther, Y., Gerlinger, B., Linke, F., Wolters, F., Vieweg, M., Krüger, W. R., Blinstrub, J. (2020). Entwurf und Bewertung einer lärmarmen Kurzstreckenkonfiguration im Vorentwurf: Erkenntnisse aus dem DLR-Projekt KonTeKst. Deutscher Luft- und Raumfahrtkongress 2020
- [5] Spakovszky, Z. S. "Advanced low-noise aircraft configurations and their assessment: past, present, and future." CEAS Aeronautical Journal 10.1 (2019): 137-157
- [6] Diedrich, A., Hileman, J., Tan, D., Willcox, K., & Spakovszky, Z. (2006, January). Multidisciplinary design and optimization of the silent aircraft. In 44th AIAA aerospace sciences meeting and exhibit (p. 1323)
- [7] Liebeck, R. H. (2004). Design of the blended wing body subsonic transport. Journal of aircraft, 41(1), 10-25
- [8] Airbus, "VELA: Very Efficient Large Aircraft," 2006
- [9] NACRE Final Activity Report, 2011
- [10] Hasan, Y. J., Schwithal, J., Pfeiffer T., Liersch, C.M., Looye, G. Handling qualities assessment of a blended wing body configuration under uncertainty considerations. Deutsche Gesellschaft für Luft- und Raumfahrt-Lilienthal-Oberth eV, German Aerospace Congress, München, Germany, 2018
- [11] Fröhler, B., Iwanizki, M., & Zill, T. (2022). Conceptual Design of a Blended-Wing-Body for a Short/Medium Range Mission Enhanced by High-Fidelity Aerodynamics.
- [12] Spakovszky, Z. S. "Advanced low-noise aircraft configurations and their assessment: past, present, and future." CEAS Aeronautical Journal 10.1 (2019): 137-157
- [13] Thomas, R. H., Burley, C. L., & Nickol, C. L. (2016). Assessment of the noise reduction potential of advanced subsonic transport concepts for NASA's Environmentally Responsible Aviation Project. In 54th AIAA Aerospace Sciences Meeting (p. 0863)
- [14] Seider, D., Fischer, P. M., Litz, M., Schreiber, A., and Gerndt, A. (eds.), Open Source Software Framework for Applications in Aeronautics and Space, IEEE Aerospace Conference, Montana, USA, 2012
- [15] Wöhler, S., Atanasov, G., Silberhorn, D., Fröhler, B., and Zill, T. (eds.), Preliminary Aircraft Design within a Multidisciplinary and Multifidelity Design Environment, Aerospace Europe Conference 2020, Bordeaux, France, 2020
- [16] Silberhorn, D., "AMC – Aircraft Mission Calculator: Documentation," 2020
- [17] Liersch, C., & Wunderlich, T. (2008, September). A fast aerodynamic tool for preliminary aircraft design. In 12th AIAA/ISSMO Multidisciplinary Analysis and Optimization Conference (p. 5901)
- [18] K. H. Horstmann, Ein mehrfach-traglinienverfahren und seine Verwendung für Entwurf und Nachrechnung nichtplanarer Flügelanordnungen, tech. rep., Deutsches Zentrum für Luft- und Raumfahrt e.V, 1987
- [19] Raymer, D. P., Aircraft Design: A Conceptual Approach (AIAA Education Series), American Institute of Aeronautics & Astronautics; 6. Edition, 2018
- [20] Kruse, Martin, Tobias Wunderlich, and Lars Heinrich. "A conceptual study of a transonic NLF transport aircraft with forward swept wings." 30th AIAA Applied Aerodynamics Conference. 2012

- [21] Fröhler, B., Hesse, C., Atanasov, G., & Wassink, P. (2021). Disciplinary Sub-Processes to Assess Low-Speed Performance and Noise Characteristics within an Aircraft Design Environment. Deutsche Gesellschaft für Luft-und Raumfahrt-Lilienthal-Oberth eV
- [22] Reitenbach, S., Vieweg, M., Becker, R., Hollmann, C., Wolters, F., Schmeink, J., Otten, T., and Siggel, M., Collaborative Aircraft Engine Preliminary Design using a Virtual Engine Platform, Part A: Architecture and Methodology, AIAA SciTech Forum 2020, Orlando, USA, 2020
- [23] CentaurSoft, Centaur Hybrid Grid Generation System, online web site, URL: <http://www.centaursoft.com>, retrieved 19<sup>th</sup> November 2012
- [24] Gerhold, T., MEGAFLOW - Numerical Flow Simulation for Aircraft Design, Springer-Verlag GmbH, Oct. 2006
- [25] Kroll, N., Langer, S., Schwöppe, A., The DLR flow solver TAU - status and recent algorithmic developments, in 52nd Aerospace Sciences Meeting, American Institute of Aeronautics and Astronautics, Jan. 2014
- [26] Spalart, P. R., Allmaras, S. R., A One-Equation Turbulence Model for Aerodynamic Flows, in 30<sup>th</sup> Aerospace Sciences Meeting and Exhibit, Reno, NV, USA, 1992
- [27] Spalart, P. R., Shur, M., On the Sensitization of Turbulence Models to Rotation and Curvature, in Aerospace Science and Technology, 1(5), pp. 297 – 302, 1997
- [28] Hasan, Y. J., Flink, J., Freund, S., Klimmek, T., Kuchar, R., Liersch, C. M., Looye, G., Moerland, E., Pfeiffer, T., Schrader, M. and Zenkner, S., “Stability and Control Investigations in Early Stages of Aircraft Design”, 2018 Applied Aerodynamics Conference, Atlanta, Georgia, USA, June 2019, DOI: <https://doi.org/10.2514/6.2018-2996>
- [29] Kiehn, D., Autenrieb, J. and Fezans, N., “COAST – A Simulation and Control Framework to Support Multidisciplinary Optimization and Aircraft Design With CPACS”, 33rd Congress of the International Council of the Aeronautical Sciences, ICAS, Stockholm, Sweden, September 2022, to be published
- [30] Ehlers, J., “Flying Qualities Analysis of CPACS Based Aircraft Models - HAREM V2.0”, DLR, Internal Report 111-2013/21, 2013
- [31] Lummer, M., Aircraft noise generation and assessment – Installation: numerical investigation. CEAS Aeronautical Journal 10, (2019): 159-178
- [32] Blinstrub, J.: Immission-based noise reduction within conceptual aircraft design. DLR Forschungsbericht, ISRN DLR-FB-2019-12 (2019). [https://doi.org/10.34912/fl8ght\\_n01s3](https://doi.org/10.34912/fl8ght_n01s3)
- [33] Bertsch, L.: Noise prediction within conceptual aircraft design. DLR Forschungsbericht, ISRN DLR-FB-2013-20 (2013). <https://doi.org/10.34912/n0is3-d3sign>
- [34] Lummer, M.: Maggi-Rubinowicz diffraction correction for ray-tracing calculations of engine noise shielding. In: 14th AIAA/CEAS Aeroacoustics Conference (29th AIAA Aeroacoustics426 J. Blinstrub et al. Conference), Vancouver, British Columbia, Canada (2008). <https://doi.org/10.2514/6.2008-3050>
- [35] Nöding, M.; Bertsch, L. Application of Noise Certification Regulations within Conceptual Aircraft Design. Aerospace 2021, 8, 210. <https://doi.org/10.3390/aerospace8080210>
- [36] Airbus S.A.S., „A320 Aircraft Characteristics - Airport and Maintenance Planning“ 2020
- [37] International Civil Aviation Organization, DOC 8168; Aircraft Operations; Volume 1, Flight Procedures; 5th Edition, 2006
- [38] Civil Aviation Organization, Annex 14; Aerodromes; Volume 1; 5th Edition, 2009
- [39] Pott-Pollenske, Michael, Almonait, Daniela, Buchholz, Heino "Low Noise ATRA–An Aircraft Noise Reduction Study based on Retro-Fit Technologies." AIAA AVIATION 2021 FORUM. 2021
- [40] David T. Chan, John R. Hooker, Andrew T. Wick, Ryan Plumley, Cale Zeune, Michael V. Ol and Joshua A. DeMoss. "Transonic Semispan Aerodynamic Testing of the Hybrid Wing Body with Over Wing Nacelles in the National Transonic Facility," AIAA 2017-0098. 55th AIAA Aerospace Sciences Meeting, January 2017
- [41] Bertsch, L., Simons, D. G., & Snellen, M. (2015). Aircraft Noise: The major sources, modelling capabilities, and reduction possibilities. <https://doi.org/10.34912/ac-n0is3>